On hurricane parametric wind and applications in storm surge modeling

Ning Lin[1] and Daniel Chavas[1]

Received 7 November 2011; revised 30 March 2012; accepted 10 April 2012; published 15 May 2012.

[1] This study revisits the parametric modeling of the hurricane surface wind field composed of the storm vortex and the environmental background flow. First, we investigate the parametric representation of the surface background wind by analyzing its empirical relationship with storm movement. A marked deceleration and counter-clockwise rotation of the surface background wind from the storm translation vector is detected, a result predicted by the Ekman theory but rarely applied in wind and surge modeling. Then, we examine the various parameters used to model the wind field and, through numerical simulations, quantify their induced uncertainties in the extreme wind and surge estimates at two coastal sites. Our analyses show that, over the range of accepted values and methods in the literature, the local wind and surge estimates are most sensitive to uncertainties in the surface wind reduction factor and storm wind profile but less sensitive to uncertainties in other wind parameters, such as inflow angle and surface background wind (varying in the observed range). The surge is more sensitive than the wind to uncertainties in the wind parameters, and these sensitivities are comparable to the sensitivity of the surge to the uncertainty in the sea surface drag coefficient. We also find that some commonly used wind parameters unsupported by theory or observations can induce significant errors in the wind and surge estimates. The results of this study provide new insights and references for future hurricane wind and surge analysis.

Citation: Lin, N., and D. Chavas (2012), On hurricane parametric wind and applications in storm surge modeling, *J. Geophys. Res.*, *117*, D09120, doi:10.1029/2011JD017126.

1. Introduction

[2] Numerical modeling of hurricane wind fields has been commonly applied in extreme wind and surge prediction and risk assessment [*Vickery et al.*, 2009a]. A storm surge is induced by the storm surface wind stress and atmospheric pressure perturbations. Since the effect of pressure is relatively small, surges are mainly driven by the wind stress, especially over shallow water in coastal areas [*Flather*, 2001]. Surge prediction, therefore, is very sensitive to wind estimation. When observed wind fields are used, state-of-the-art storm surge models can often produce successful hindcasts of surges [e.g., *Houston et al.*, 1999, *Westerink et al.*, 2008; *Bunya et al.*, 2010]. In real-time forecasting, predictions of winds, and thus surges, can be performed using advanced numerical weather forecasting models [e.g., *Colle et al.*, 2008; *Lin et al.*, 2010a]. Alternatively, parametric hurricane wind models are more frequently used due to their simplicity and efficiency, especially in long-term wind and surge risk assessment and structural design [*Vickery et al.*, 2009a; *Lin et al.*, 2010b, 2012].

[3] In the parametric approach, the surface wind field may be estimated as the sum of an axisymmetric wind field associated with the storm itself and a background wind field of the environment. The surface background wind is often related to the storm's translation velocity, based on two assumptions: the storm's movement is mainly due to advection by (some vertically integrated measure of) the background wind in the free troposphere near the storm [*Chan*, 2005], and the surface friction causes the surface background wind to deviate from the free tropospheric wind in magnitude and direction. However, absent adequate data, disagreement remains regarding the nature of this deviation. Some previous applications assumed that the surface background wind is approximately equal in direction to the storm translation velocity and reduced in magnitude by a factor of various values (e.g., 0–0.5 used by *Jelesnianski et al.* [1992] and *Phadke et al.* [2003], 0.6 by *Emanuel et al.* [2006], and 0.5 by *Lin et al.* [2012]). In many other applications, the full velocity of the storm's translation is added to the storm's wind field [e.g., *Powell et al.*, 2005; *Mattocks and Forbes*, 2008; *Vickery et al.*, 2009b], neglecting the velocity difference between the free tropospheric wind and surface

[1]Department of Earth, Atmospheric, and Planetary Sciences, Massachusetts Institute of Technology, Cambridge, Massachusetts, USA.

Corresponding author: N. Lin, Department of Earth, Atmospheric, and Planetary Sciences, Massachusetts Institute of Technology, Cambridge, MA 02139-4307, USA. (ninglin@mit.edu)

0148-0227/12/2011JD017126

background wind. A poor representation of the background wind component of the wind field may cause significant underestimation or overestimation of the wind and surge; therefore, the actual relationship between the surface background wind and storm movement needs to be investigated.

[4] Given storm characteristics (i.e., track, intensity, and size), the axisymmetric component of the surface wind may be estimated by calculating the wind velocity at gradient level with a hurricane wind profile and translating the gradient wind to the surface level with an empirical surface wind reduction factor (SWRF) [*Powell et al.*, 2003] and inflow angle [e.g., *Bretschneider*, 1972] to account for the effect of surface friction on the storm. (A boundary layer model [e.g., *Thompson and Cardone*, 1996; *Vickery et al.*, 2009b; *Kepert*, 2010] may be applied to more accurately calculate the surface wind from the gradient condition, but it is nonparametric and more computationally expensive.) A number of gradient wind profiles [e.g., *Holland*, 1980; *Jelesnianski et al.*, 1992; *Emanuel*, 2004] have been widely used in wind and surge analysis, but the wind and surge calculated using these profiles have yet to be compared in a statistical sense (though case studies do exist [e.g., *Phadke et al.*, 2003]). Although it may be difficult at this point to identify the "best" wind profile, as each profile has its own strengths and limitations, the knowledge of how wind and surge estimates vary with different profiles is necessary in uncertainty analysis. It is also useful to investigate the sensitivities of wind and surge estimates to the effect of surface friction on the storm, for example, by examining the sensitivities to SWRF and inflow angle, the values of which have not been agreed upon [*Vickery et al.*, 2009a] and may vary with storm conditions and wind speeds [*Powell et al.*, 2005].

[5] This paper revisits hurricane parametric wind modeling and discusses its application in wind and surge risk assessment. We first exploit the Hurricane Research Division H*Wind tropical cyclone surface wind database [*Powell et al.*, 1998] and the Best Track database (updated from *Jarvinen et al.* [1984]) to establish empirical relationships between the storm movement and surface background wind. To our knowledge, this is the first effort to explore this issue directly from observations. Then, through numerical simulations, we study the sensitivities of the wind and surge estimates to various wind model parameters: the representation of the surface background wind, gradient wind profile, SWRF, and inflow angle. As a comparison, we also investigate the sensitivity of the surge estimates to the sea surface drag coefficient (C_d), which determines the surface wind stress given the wind velocity and thus is a critical parameter in surge modeling.

[6] Specifically, we apply the Advanced Circulation (ADCIRC) model [*Luettich et al.*, 1992; *Westerink et al.*, 1992] to simulate the surges induced by large numbers of synthetic storms generated from the statistical/deterministic hurricane model of *Emanuel et al.* [2006] (details of the method are given by *Lin et al.* [2012]). We apply accepted ranges in the literature of the above mentioned parameters and carry out sensitivity analysis for two coastal sites. The first site is New York City (NYC), whose vulnerability to storm surge is sensitive to its location at the vertex of the right angle made by Long Island and New Jersey [*Colle et al.*, 2008; *Lin et al.*, 2010b, 2012]. The other is Tampa, Florida, which is rendered perhaps even more vulnerable to storm surge due to its geophysical features: it is surrounded by low-lying lands and affected by (surge-induced) edge waves trapped on the west Florida shelf [*Weisberg and Zheng*, 2006; *Yankovsky*, 2009]. Note that we focus on the sensitivity of wind and surge estimates to the wind (-field) parameters; the storm characteristics may be estimated from observations [e.g., Best Track and H*Wind data], from forecasts [e.g., *Kurihara et al.*, 1998], or from statistical [*Vickery et al.*, 2000] or statistical/deterministic [*Emanuel et al.*, 2006, 2008] synthetic hurricane simulations. The uncertainties of wind and surge estimates due to the uncertainties in the characteristics of the storm itself can also be of similar or even greater magnitude [*Irish et al.*, 2008; *Rego and Li*, 2009]; these uncertainties will be investigated in a future study.

[7] In Section 2, we introduce the method to estimate the surface background wind and obtain its empirical relationships with storm movement. In Section 3, we present the simulated peak wind speeds and surge heights at NYC and Tampa and examine their sensitivities to five surface background wind representations (based on Section 2), four gradient wind profiles [*Holland*, 1980; *Jelesnianski et al.*, 1992; *Emanuel*, 2004; *Emanuel and Rotunno*, 2011], four values of SWRF (0.7, 0.8, 0.85 and 0.9), two empirical expressions of inflow angle (used by the National Weather Service (NWS) [*Bretschneider*, 1972] and by *Queensland Government* [2001], respectively), and two formulae of C_d (*Garratt* [1977] and *Large and Pond* [1981], modified based on *Powell et al.* [2003]). Section 4 discusses significant errors that may be induced by using incorrect wind parameters. Section 5 summarizes the paper with recommendations for future applications of parametric winds in hurricane wind and surge analysis.

2. Surface Background Wind Estimation

[8] To establish a reasonable representation of the surface background wind, we perform an observational analysis to estimate statistically the magnitude and orientation of the surface background wind relative to the storm translation velocity. The methodology is based upon the vector decomposition of the surface wind field into an axisymmetric component of the storm vortex and an axially asymmetric component of the surface background wind. Suppose the surface background wind is decelerated by a factor, α, and rotated counter-clockwise (in the Northern Hemisphere) by an angle, β, from the free tropospheric wind that advects the storm, based on the Ekman boundary layer theory. We note that in reality the background flow may be affected by the existence of the storm vortex and thus may not be uniform over the storm wind field; one would not expect α and β to remain constant over the storm domain, an aspect that we explore below. Although α and β may also vary, for example, with background wind speed and latitude (e.g., due to extratropical transition), no obvious trend is detected in the observational database; we estimate the mean values of these parameters over all available surface wind fields. Further, in reality, tropical cyclones are not perfectly symmetric [e.g., *Frank and Ritchie*, 1999; *Shea and Gray*, 1973], and the storm's internal asymmetry will likely bias the calculated background wind parameters. Nevertheless,

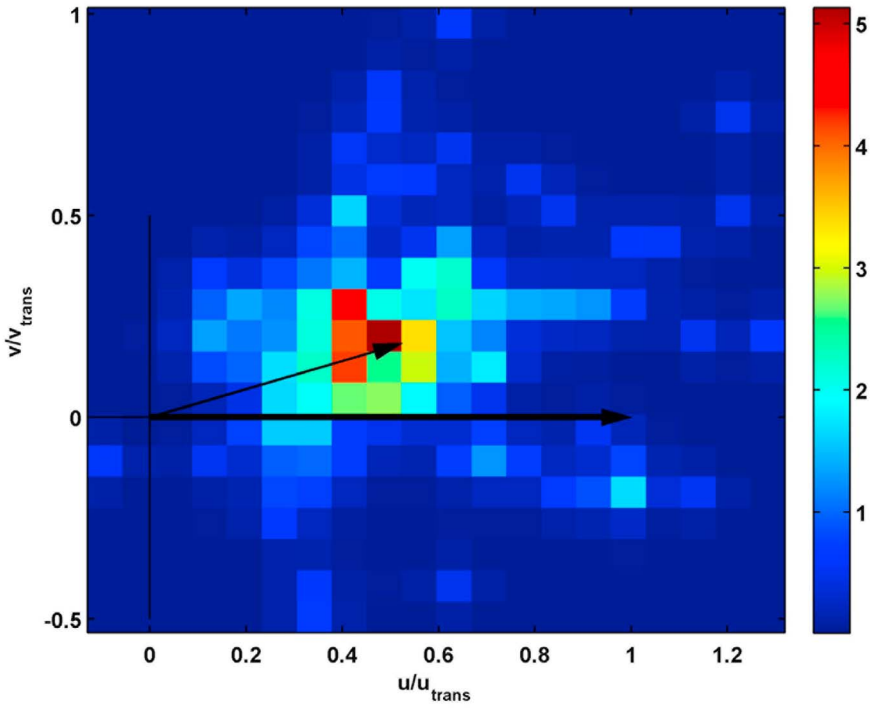

Figure 1. Spatial frequency distribution (colors) of the normalized surface background wind vector (from 147 snapshots in the H*Wind database), relative to the standardized unit translation vector depicted here with an arbitrary westerly orientation, for a storm-centered box with side length L = 600 km. The mean of the wind vector (upper black arrow) is equal to the unit translation vector whose magnitude is reduced by a factor α = 0.56 and which is rotated counter-clockwise by an angle β = 19.2°.

here we assume that residual internal asymmetries in the vortex flow are randomly oriented from storm to storm and in time, and the statistical mean of α and β for a large sample of wind fields will asymptotically approach their expected values absent other asymmetries in the flow field.

[9] We use all observed surface wind fields (at 10 m) in the Hurricane Research Division H*Wind Atlantic basin storm data sets for the years 1998–2009 (1583 8° × 8° wind field snapshots at approximately 6-km horizontal resolution). Storms within this data set are located primarily in the Western Atlantic, Caribbean, and Gulf of Mexico, where aircraft reconnaissance of wind structure is common, thereby lending high confidence in the final H*Wind product (for product details, see *Powell et al.* [1998]). The results are filtered for cases that satisfy the following conditions: (i) translation speed > 4 m/s to ensure a sufficiently strong translation signal; (ii) maximum wind speed > 40 m/s to ensure a well-defined center of circulation; (iii) <1% land in the domain (H*Wind reduces wind speeds over land, which introduces asymmetry); and (iv) acceleration vector magnitude < 10^{-4} m/s^2 to ensure nearly steady background flow in the vicinity of the storm. The storm translation velocity is calculated for each storm from a cubic spline interpolation of the Best Track data (updated from *Jarvinen et al.* [1984]) to the analysis time.

[10] In the analysis, we first assume the surface background flow to be relatively uniform over the storm domain (i.e., α and β constant over the wind field), so that it is approximately equal to the mean of the surface wind over a storm-scale rectangular area centered at the storm center as determined by the H*Wind analysis procedure (note: the mean of the axisymmetric component including the surface friction effect vanishes). For each wind field, we calculate the background wind vector within a storm-centered box with side length L and define its magnitude and orientation relative to the translation vector (normalization). The translation vectors for all analysis wind fields are then reoriented and rescaled to a common unit vector, thereby creating a statistical composite of the normalized background wind vectors relative to this common translation vector. The (2D) spatial frequency distribution of the normalized background wind vector is then obtained, and the mean values of parameters α (magnitude) and β (direction of the vector) are estimated. We perform this analysis with a range of box sizes comparable to the storm scale and up to 800 km, approximately the domain size of the H*Wind wind field products. As an example, the results for box side length L = 600 km are displayed in Figure 1, with estimated mean deceleration factor α = 0.56 and mean angle of rotation β = 19.2°. Clearly there is a marked deceleration of the storm translation to the surface background wind; the storm often moves much faster than the surface background wind. Also, there is a distinct counter-clockwise rotation of the translation vector to the surface level which should not be neglected if one seeks to more accurately represent the flow field in the hurricane boundary layer.

[11] However, the values of α and β are somewhat sensitive to the box size, suggesting a dependence of each on

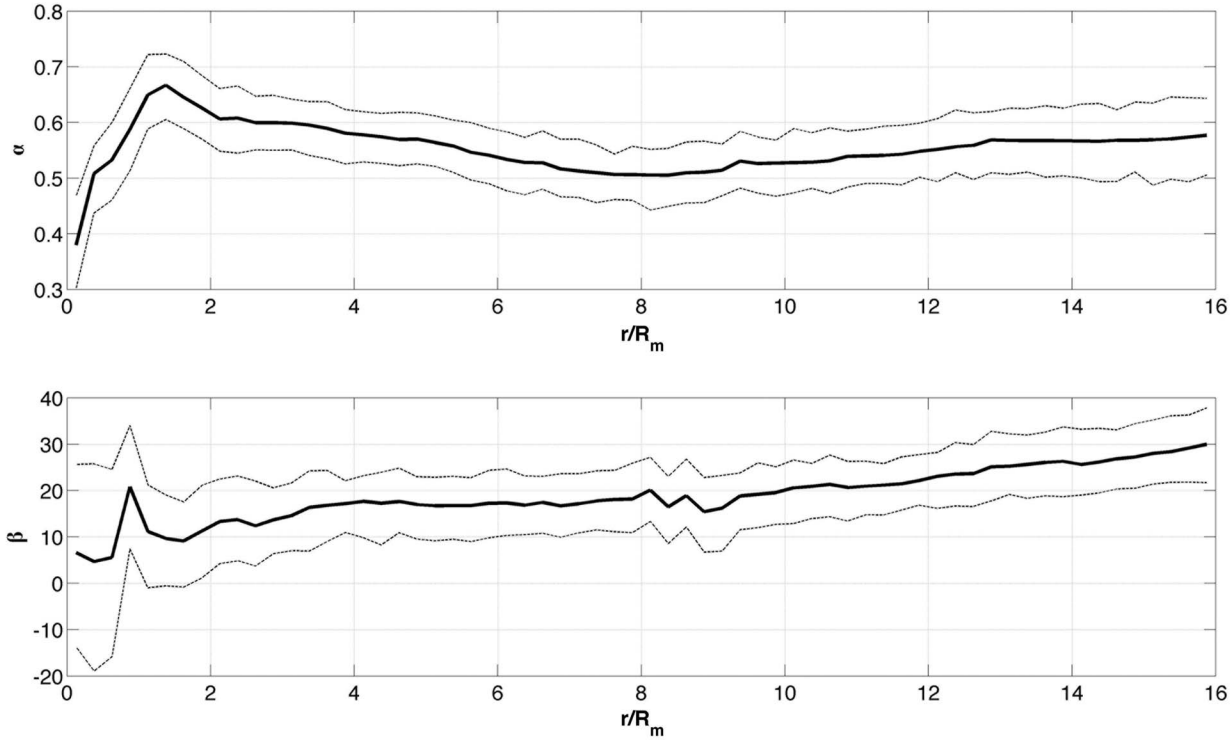

Figure 2. Estimated mean values (thick solid lines) of storm translation to surface background wind reduction factor, (top) α, and counter-clockwise rotation angle, (bottom) β, as a function of radius normalized by the radius of maximum wind. 95% confidence intervals (thin dashed lines) are calculated using a bootstrap method with 100 re-samples at each value of non-dimensional radius.

radius from storm center. Thus, we calculate α and β as functions of radius normalized by the radius of maximum wind (R_m; obtained from the azimuthal-mean total wind as a function of radius in 5-km bins). The analysis method is identical to that described above except it is applied within storm-centered rings at equally spaced intervals of normalized radius. The result is shown in Figure 2. The deceleration factor α increases with radius until reaching a maximum of 0.67 at a radius $r = 1.38R_m$ and then decays gradually with radius to 0.51 at $r = 8R_m$ before increasing again to 0.57 at $r = 13R_m$. The rotation angle β exhibits a weaker radial dependence outside the eyewall; it ranges from a minimum 9.1° at $r = 1.63R_m$ to 20° at $r = 10R_m$, and then gradually increasing above 20° at larger non-dimensional radii. β varies greatly in the inner core; however, the large error bars for $r < 2R_m$ render questionable any claims of a robust radial dependence. These large variations and error bars may also result from the internal asymmetries of the vortex flow oriented in a systematic (i.e., non-random) manner [*Shea and Gray*, 1973], which have been shown to be larger in the storm's inner core [*Weatherford and Gray*, 1988].

[12] In practice, one may ignore the relatively small radial dependence of the parameters. We elect to set $\alpha = 0.55$ and $\beta = 20°$, considering that in the Atlantic basin the median storm size as measured by the storm's outer radius (the radius of vanishing winds) is approximately 400 km [*Chavas and Emanuel*, 2010] or $r \sim 10R_m$ for typical values of R_m. Indeed, as shown in the next section, wind and surge estimates are not very sensitive to the radial variation of α and β in the main observational ranges of 0.5–0.6 and 15°–22°, respectively.

3. Uncertainties in Parametric Wind and Surge Analysis

[13] We apply two large data sets of synthetic storms that pass by NYC (5000 storms) and Tampa (3000 storms), respectively, generated from the statistical/deterministic hurricane model of *Emanuel et al.* [2006], for the climate during the years 1981–2000 estimated from the National Center for Environmental Prediction/National Center for Atmospheric Research (NCEP/NCAR) reanalysis [*Kalnay et al.*, 1996]. Note that in this sensitivity/uncertainty study, we use synthetic storms rather than hypothetical storms; all storms are realistic and have physically correlated characteristics. We focus on the extremes that determine the risk and select 295 of the most intense storms for NYC and 135 of the most intense storms for Tampa; the selected storm set for each site encompasses all synthetic storms that have estimated return periods greater than 50 years in the original storm data sets for the NCEP/NCAR climate condition.

[14] We apply the ADCIRC model [*Luettich et al.*, 1992; *Westerink et al.*, 1992] to simulate the surge induced by the selected storms. For NYC, the surge-simulation mesh is an unstructured grid developed by *Lin et al.* [2012] with a resolution of approximately 100 m around NYC and up to 100 km over the deep ocean. The ADCIRC parameters are set to follow those of *Colle et al.* [2008], whose results

were validated against observations for the NYC area. For Tampa, the simulation mesh, modified from a mesh of *Blain et al.* [1994], covers the entire Gulf of Mexico and has a resolution of approximately 600 m around Tampa Bay. The ADCIRC parameters are set to follow those of *Westerink et al.* [2008], whose results were validated against observations for the Gulf area. Both of the numerical meshes are confined to the open ocean and we focus on the coastal surge. To be consistent, we present the simulated peak wind speeds and surge heights (over the storm lifetime) at the same coastal locations: the Battery, NYC (74.02 W, 40.9 N) and the City of Tampa (82.46 W, 27.89 N). The presented peak wind is the 1-min. average wind at 10 m over ocean-like surface roughness. For the ADCIRC surge simulations, the 1-min. wind is adjusted to a 10-min. average by a reduction factor of 0.893 [*Powell et al.*, 1996], and the storm surface pressure is estimated from the pressure model of *Holland* [1980].

[15] To study the uncertainties in parametric winds and the sensitivities of surge responses, we define a control case and investigate how wind and surge estimates vary with each parameter when other parameters are controlled. The parameters used for the control case are: surface background wind parameters $\alpha = 0.55$ and $\beta = 20°$, the *Emanuel and Rotunno* [2011] wind profile (used by [*Lin et al.*, 2012] in surge analysis), SWRF = 0.85 [*Batts et al.*, 1980], NWS's expression of inflow angle [*Bretschneider*, 1972], and *Garratt*'s [1977] expression of C_d, capped at 0.0025 [*Powell et al.*, 2003]. Each of these parameters is introduced with wind and surge sensitivity analysis in the following subsections. The wind and surge sensitivities are expressed as the deviation (%) from the control case for the varied parameter; the mean, median, and range of the deviation over all selected storms for each location and for each parameter are shown. The deviations of each case from all other cases are also calculated, and the largest mean deviation (variation), indicating the overall uncertainty range, is presented.

3.1. Surface Background Wind

[16] In Section 2, we suggest using the storm translation to surface background wind reduction factor, $\alpha = 0.55$, and counter-clockwise rotation angle, $\beta = 20°$, to estimate the surface background wind. Here we test if the wind and surge estimates are sensitive to these two parameters varying between 0.5–0.6 and 15°–22°, respectively, which were identified as the main ranges of radial variation (Figure 2). Figure 3 compares the wind and surge estimates using $(\alpha, \beta) = (0.5, 20°)$, $(\alpha, \beta) = (0.6, 20°)$, $(\alpha, \beta) = (0.55, 15°)$, and $(\alpha, \beta) = (0.55, 22°)$ respectively, with those using control values $(\alpha, \beta) = (0.55, 20°)$. Increasing α (from 0.55 to 0.6) often increases the peak wind (with a mean deviation of 0.46% for NYC and 0.65% for Tampa) and peak surge (1.9% for NYC and 1.4% for Tampa), but in some cases it decreases the (peak) wind when they are generated from the wind fields to the left of the storms where the background wind reduces the magnitude of the total wind; vice versa for the decreasing of α (from 0.55 to 0.5). While increasing β (from 20° to 22°) often increases the wind (0.42% for NYC and 0.085% for Tampa), it increases the surge for NYC (0.6%) but decreases the surge for Tampa (−0.26%); vice versa for the decreasing of β (from 20° to 15°). This difference between the two sites may be due to their geographical features: the majority of the storms affecting NYC move northward along the Atlantic coast and the effect of β in these storms usually pushes water into New York Harbor, but storm tracks affecting Tampa have larger variations and the effect of β in storms that pass northward along the west Florida coast often moves water away from Tampa Bay.

[17] Over all, the differences in the wind and surge estimates for α and β varying within the main observational ranges are relatively small, with the largest mean variation of the wind estimates to be 0.9% for NYC and 1.3% for Tampa and the largest mean variation of the surge estimates to be 4% for NYC and 2.9% for Tampa. This smallness in variation is because for extreme events the wind field is dominated by the component associated with the storm itself, and thus the relatively small changes in the background wind induce small changes in the wind and surge estimates. However, as discussed in Section 4, greater changes in the background wind parameters can still induce significant over- or under- estimation of the wind and surge for extreme events. In addition, it is noted that surge estimates are more sensitive than wind estimates. As shown in the following analysis, this difference in wind and surge sensitivities is general with respect to all wind parameters, because the (peak) wind is determined by the wind field at a particular moment at the site while the (peak) surge is induced by the cumulative nonlinear effect of the wind stress (a quadratic function of the wind speed) over space and time.

3.2. Gradient Wind Profile

[18] We study four gradient wind profiles, using the storm characteristics along storm tracks generated by the synthetic hurricane model: the storm central pressure deficit (ΔP), symmetrical maximum wind speed (V_m), radius of maximum wind (R_m), and outer radius (R_o). The *Holland* [1980] wind profile (hereafter H80) is most widely used and is based on an empirical radial distribution of the storm pressure and the assumption of gradient wind balance. The gradient wind velocity, V, at a radius r is given by

$$V(r) = \left\{ \left(\frac{R_m}{r}\right)^B \frac{B\Delta P e^{\left[-\left(\frac{R_m}{r}\right)^B\right]}}{\rho} + \frac{r^2 f^2}{4} \right\}^{\frac{1}{2}} - \frac{fr}{2}, \qquad (1)$$

where e is the base of natural logarithms, ρ is the air density, f is the Coriolis parameter ($f = 2\Omega\sin\varphi$, where $\Omega = 7.292 \times 10^{-5}$ and φ is the latitude), and B is the Holland parameter,

$$B = \frac{V_m{}^2 e\rho + f V_m R_m e\rho}{\Delta P}. \qquad (2)$$

Since the Coriolis force is relatively small in the region of maximum winds, the cyclostrophic approximation has often been applied, neglecting the terms associated with f in equations (1) and (2) (hereafter H80c). However, the cyclostrophic approximation may induce inaccurate wind estimation away from the region of maximum winds and thus inaccurate local wind and surge estimates. It is also important to note that the cyclostrophic form of equation (2) is derived from the cyclostrophic form of equation (1). Using the cyclostrophic form of equation (2) together with the gradient wind-balance form of equation (1), as in many previous

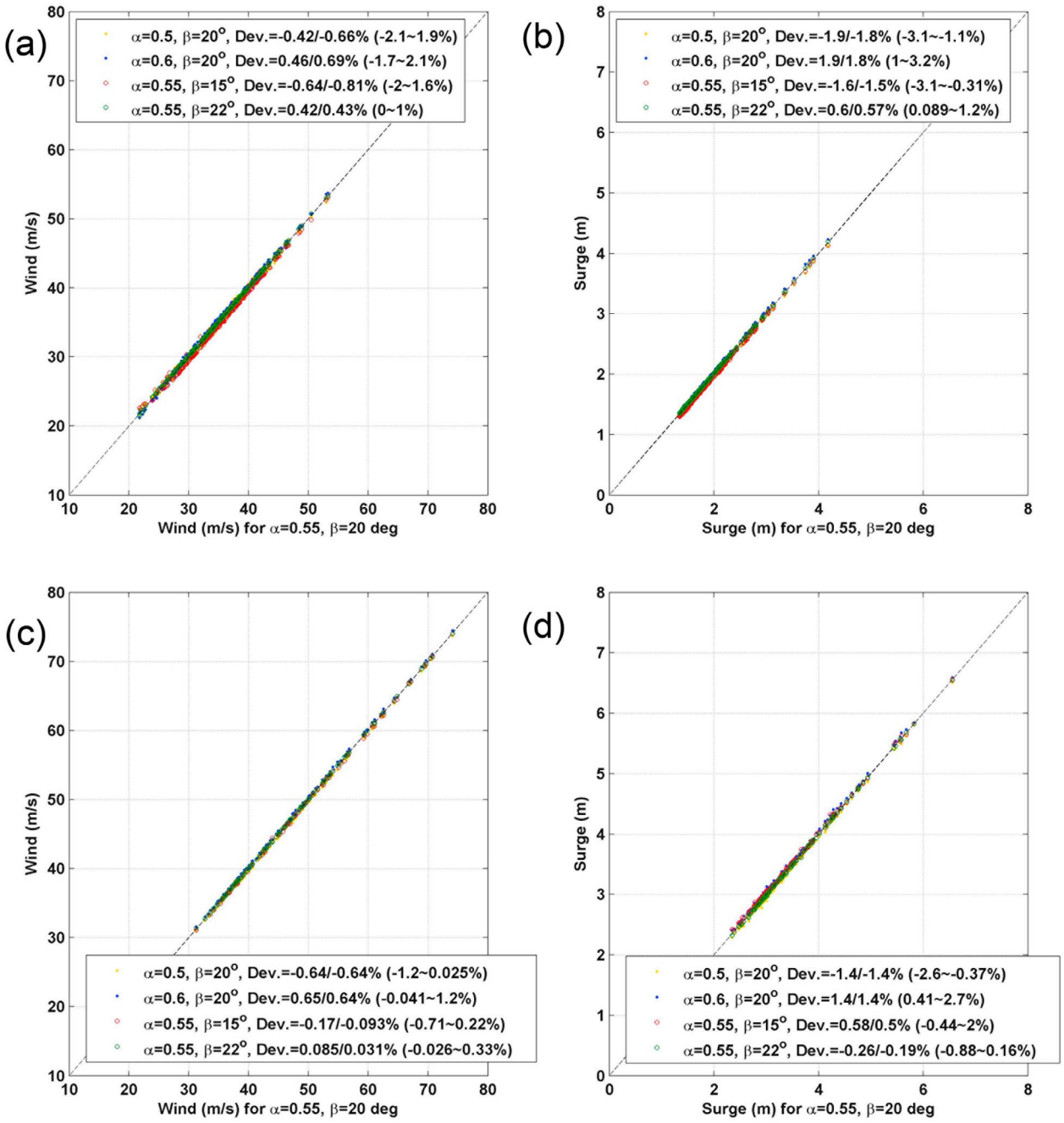

Figure 3. Comparison of the wind and surge estimates using various values of the surface background wind reduction factor, α, and counter-clockwise rotation angle, β, over the observed ranges, with those of the control case using α = 0.55 and β = 20, for (a and b) NYC (295 storms) and (c and d) Tampa (135 storms). The wind/surge sensitivity is expressed as the deviation (%) from the control case; the mean, median, and range of the deviation over all storms for each location are displayed in the form of "Dev. = mean/median% (0.5 quantile ~ 0.95 quantile %)." The same format also applies for latter plots.

applications, will result in an underestimation of the wind speed near the radius of maximum wind (it is easy to show that the gradient wind-balance form of equation (1) will give a value of V_m that is smaller than its input value in the cyclostrophic form of equation (2)). *Holland et al.* [2010] extends H80c by allowing a variation in the wind equation exponent (1/2 in equation (1)) to fit outer wind observations. As such observational data is not always available and unavailable for synthetic storms, this profile is not applied here for sensitivity analysis. However, out of curiosity, we use another wind profile [*Emanuel and Rotunno*, 2011; see below for descriptions] to estimate the radius of the 12-m/s

wind outside R_m and apply it to the *Holland et al.* [2010] profile; then the two profiles give statistically similar wind and surge estimates (not shown).

[19] The NWS currently uses the Sea, Lake, and Overland Surges from Hurricanes (SLOSH) model [*Jelesnianski et al.*, 1992] for hurricane storm surge simulations and forecasting. The SLOSH wind profile (hereafter S92) is expressed as

$$V(r) = V_m \frac{2R_m r}{{R_m}^2 + r^2}. \quad (3)$$

This wind profile was first used by *Jelesnianski* [1966] to form a simple algebraic formulation of the wind speed for surge analysis. Although wind estimates from the entire SLOSH wind model have been compared with observations [*Houston et al.*, 1999], the wind-profile component of the model has not been evaluated.

[20] As discussed by *Emanuel* [2004], although mature hurricanes in a quasi-steady state have nearly symmetric and uniform circulations, the hurricane's structure is determined by different mechanisms in different regions. *Emanuel* [2004] developed a hurricane model that regards the wind profile in the outer region of the storm as being determined by the balance between radiatively controlled subsidence in the free troposphere and Ekman suction in the boundary layer, and the outer part of the storm's eyewall being controlled by thermal wind balance, convective neutrality in the vortex, and entropy and momentum balance in the boundary layer. He then derived asymptotic solutions of the model for each region and, by patching the solutions together and extending the asymptotic limit to the storm center (based on numerical simulations from a dynamical model), he obtained a wind profile for the entire storm structure. Validated against flight level observations, this wind profile (hereafter E04) is described, for $r \le R_o$, as

$$V(r) = V_m \frac{R_0 - r}{R_0 - R_m} \left(\frac{r}{R_m}\right)^m \cdot \left[\frac{(1-b)(n+m)}{n + m\left(\frac{r}{R_m}\right)^{2(n+m)}} + \frac{b(1+2m)}{1 + 2m\left(\frac{r}{R_m}\right)^{2m+1}}\right]^{\frac{1}{2}}, \quad (4)$$

where b, m, and n are empirical parameters governing the shape of the wind profile: $b = 0.25$, $m = 1.6$, and $n = 0.9$.

[21] *Emanuel and Rotunno* [2011] improved *Emanuel*'s [2004] model for the outer part of the storm eyewall by assuming a constant (critical) Richardson Number in the storm outflow, which determines the variation of the outflow temperature and thereby the radial structure of the storm outside its radius of maximum wind. The model was shown (by numerical simulations) to produce physically realistic results. An asymptotic solution of the model gives an analytical gradient wind profile (hereafter E11) for V ($V \ge 0$),

$$V(r) = \frac{2r\left(R_m V_m + \frac{1}{2} f {R_m}^2\right)}{{R_m}^2 + r^2} - \frac{fr}{2}, \quad (5)$$

where the ratio of the exchange coefficients for enthalpy and momentum in the original model disappear as we have assumed the two coefficients to be approximately equal in magnitude based on observations [*Powell et al.*, 2003] and sensitivity analysis [*Emanuel and Rotunno*, 2011]. This wind profile is most accurate near the radius of maximum wind but is less accurate for the outer region of the storm, where the critical Richardson Number assumption may be violated. Also, similar to other steady state models, this wind profile is not accurate near the center of the storm, as the effect of radial diffusion in the eye is not accounted for. Curiously, if the terms associated with the Coriolis parameter, f, are neglected, equation (5) becomes S92 in equation (3).

[22] For illustration, Figure 4 compares these parametric wind profiles applied to two storms: the most and least intense at landfall among the selected storms for Tampa. Moving radially outward from the center to the radius of maximum wind, R_m, azimuthal wind speed increases most rapidly in E11 and S92, followed by E04, and finally both Holland profiles. Given that E04 is the only one among these profiles that is made asymptotically consistent with dynamic solutions (that account for the effect of radial diffusion in the storm center; *Emanuel* [2004] showed a comparison), it may more accurately reproduce storm inner structure. Meanwhile, the storm structure outside R_m varies greatly among the wind profiles. In the outer region of the storm's eyewall, wind speed decreases more rapidly in the H80 and E04 profiles relative to E11 for the intense storm (Figure 4a). For the relatively weak storm (Figure 4b), the H80 profile decays more slowly with radius, approaching the E11 profile. In the outer region of the storm, E04 makes use of the information of the storm's outer radius, R_o, to define outer profiles; E11 has short profile tails and underestimates R_o; and H80 has long profile tails and lacks a well-defined R_o. S92 decays relatively slowly for the whole region outside R_m, and its R_o is ill-defined. Note that H80c gives much higher outer profile winds compared to H80, especially for the weak storm (see Figure 4b). This approximate profile is shown here for comparison; it is not used in the following sensitivity investigation as it is not recommended for wind or surge analysis in practice, but in Section 4 we will demonstrate the magnitude of errors this cyclostrophic approximation may induce if it is used.

[23] The differences in the parametric wind profiles are reflected in the differences in the peak wind and surge estimates at the sites using these profiles, as shown in Figure 5. The peak winds at the sites (Figures 5a and 5c) are often generated when the storms are relatively strong and their radius of maximum wind pass near or directly over the sites. Compared to E11, H80 and E04 often give lower peak wind estimates due to their weaker profile winds in the storm's inner and outer eyewall regions (when the storms are relatively strong). Although H80 and E04 have higher profile winds than E11 in the outer region of the storm, the peak winds at the sites usually do not come from these far wind field regions (generated when the storms are relatively far away from the sites). S92 often gives higher wind estimates, compared to E11, due to its stronger profile winds outside the radius of maximum wind. The deviations of the wind estimates using H80, E04, and S92 from those using E11 are on average small to moderate, with the mean deviations being −1%, −2.4%, and 0.6%, respectively, for NYC and −2.6%, −4%, and 0.45%, respectively, for Tampa. Over all profiles the largest mean variation of the wind estimates is

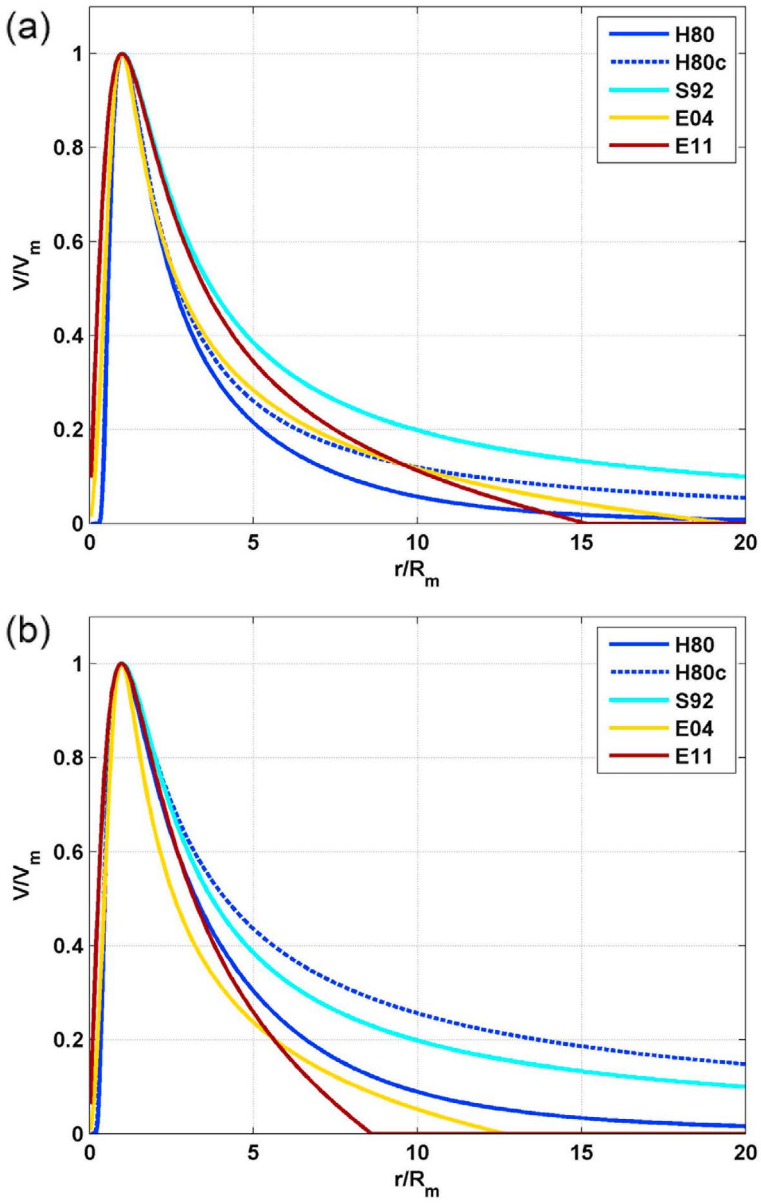

Figure 4. Comparison of parametric wind profiles (a) for a relatively intense storm and (b) for a relatively weak storm, making landfall near Tampa. The storm for Figure 4a has the following parameters: $\varphi = 28.0°$, $\Delta P = 88.3$ mb, $V_m = 80.2$ m/s, $R_m = 20.5$ km, and $R_o = 400$ km. The storm for Figure 4b has $\varphi = 28.1°$, $\Delta P = 30.3$ mb, $V_m = 39.5$ m/s, $R_m = 31.6$ km, and $R_o = 400$ km.

3.3% for NYC and 5% for Tampa, due to the deviation of the estimates using S92 from those using E04.

[24] The surge estimates (Figures 5b and 5d) are much more sensitive than the wind estimates to different wind profiles. Usually the stronger the profile winds, the larger the storm surge; and the surge is mainly determined by the inner and outer eyewall regions of the profile winds. Therefore, in most cases, the surge estimates using H80 and E04 are lower than the surge estimates using E11, with the mean deviations being −6.1% and −13%, respectively, for NYC and −6.1 and −11%, respectively, for Tampa; the surge estimates using S92 are higher than those using E11, with the mean deviations being 5.4% for NYC and 5.3% for Tampa. There exist cases, however, in which the surge estimates using H80 are higher than those using E11, with deviations greater than 4.7% for NYC and 11% for Tampa. These higher surges under H80 may be generated mainly from the moments when the storms are relatively weak so that the H80 winds are very close to the E11 winds in the outer eyewall region while the H80 winds are much stronger than the E11 winds in the farther out region of the storm (see Figure 4b). This effect does not show up in the wind estimates (Figures 5a and 5c) as the peak winds are often generated when the storms are relatively strong. Over all profiles the largest

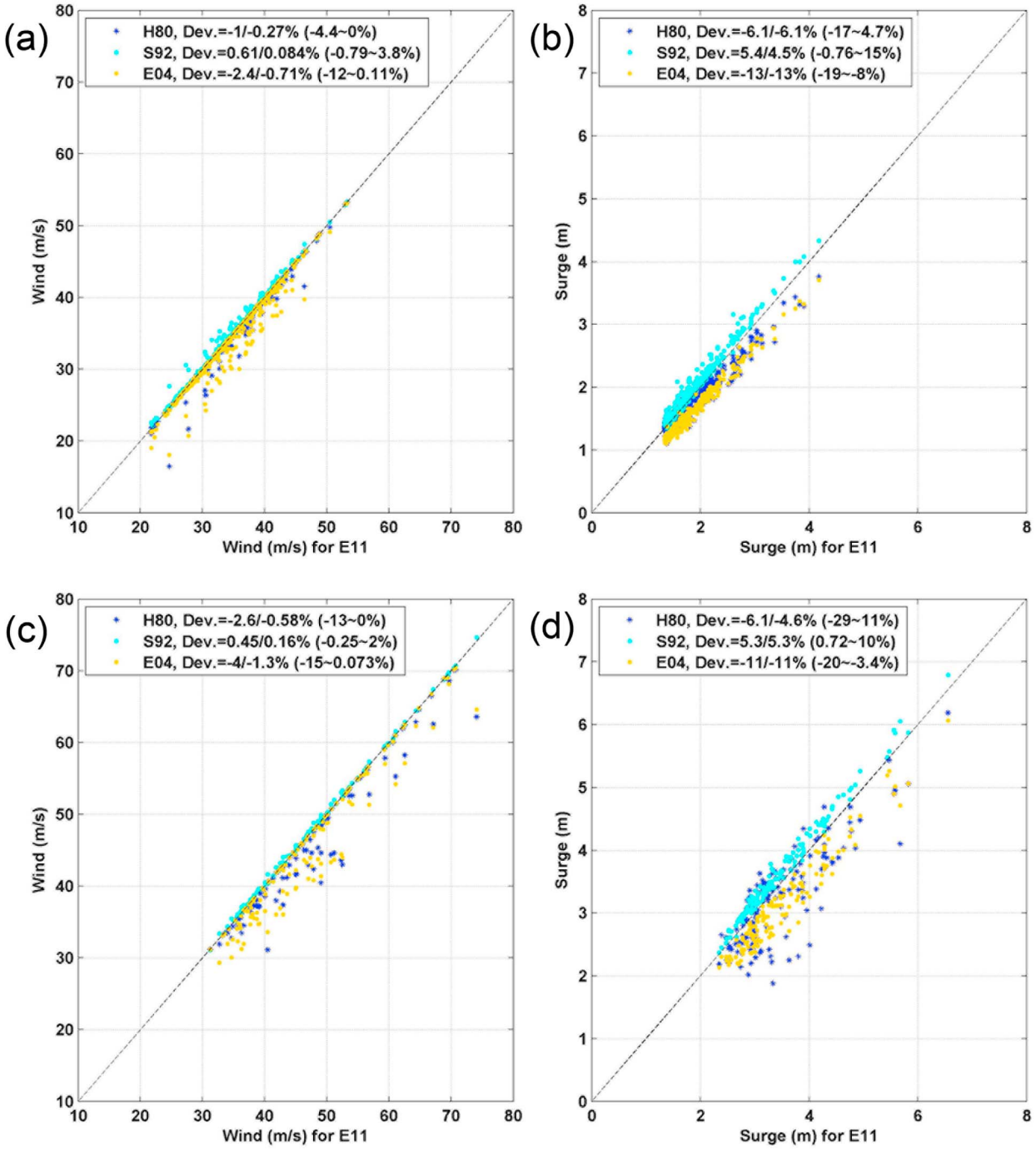

Figure 5. Comparison of the wind and surge estimates using various gradient-wind profiles with those of the control case using E11, for (a and b) NYC (295 storms) and (c and d) Tampa (135 storms).

mean variation of the surge estimates is 21.7% for NYC and 18.8% for Tampa, again due to the deviation of the estimates using S92 from those using E04.

[25] To further examine the impact of applying different wind profiles on the wind and surge estimates, we compare these estimates using each of the four wind profiles, H80, E04, S92, and E11, with the averages of these estimates over the four profiles, as shown in Figure 6. The deviations from the averages are relatively small for wind estimates (Figures 6a and 6c). Wind estimates using H80 and E11 are closest to the averages; a small number of the H80 estimates are lower than the averages and a small number of the E11 estimates are higher than the averages. Most E04 and S92 wind estimates are also very close to the averages, with some E04 estimates lower and some S92 estimates higher than the averages. Compared to the wind estimates, the deviations from the averages are much larger for the surge estimates (Figures 6b and 6d). Most E04 surge

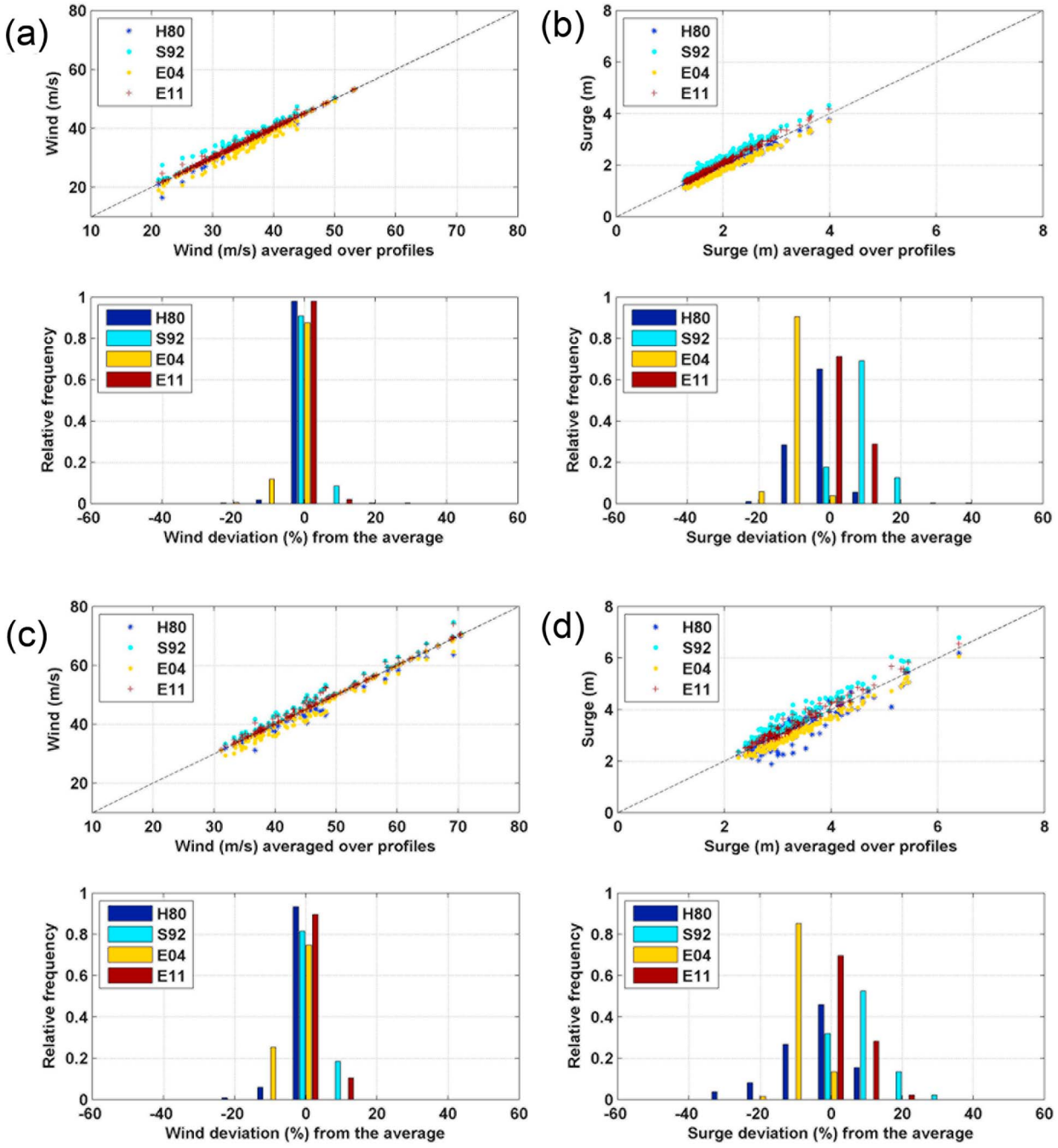

Figure 6. Comparison of the wind and surge estimates using each of the four gradient-wind profiles with the averages of the estimates over these profiles, for (a and b) NYC (295 storms) and (c and d) Tampa (135 storms). The lower panel of each subplot shows the distribution of the deviation (%) of the (wind or surge) estimates using each profile from the average of the estimates over the four profiles.

estimates are lower than the averages by about 10%, and most S92 surge estimates are higher than the averages by about 10%. H80 surge estimates have wide-spread deviations, especially for Tampa, from −30% to 10%. E11 surge estimates are most likely to be around the averages, but some E11 surge estimates are higher than the averages by about 10%. In summary, these results are consistent with those in Figures 4 and 5. Local peak wind estimates are not very sensitive to the wind profiles used, but peak surge estimates can vary greatly with the wind profiles. Since surge is mainly determined by the wind fields in the vicinity of the eyewall region, E11 is most likely to give accurate estimates as its outer eyewall structure is developed based on physical arguments and is numerically validated. Although it may overestimate the surge in some cases, as it may overestimate the winds toward the storm

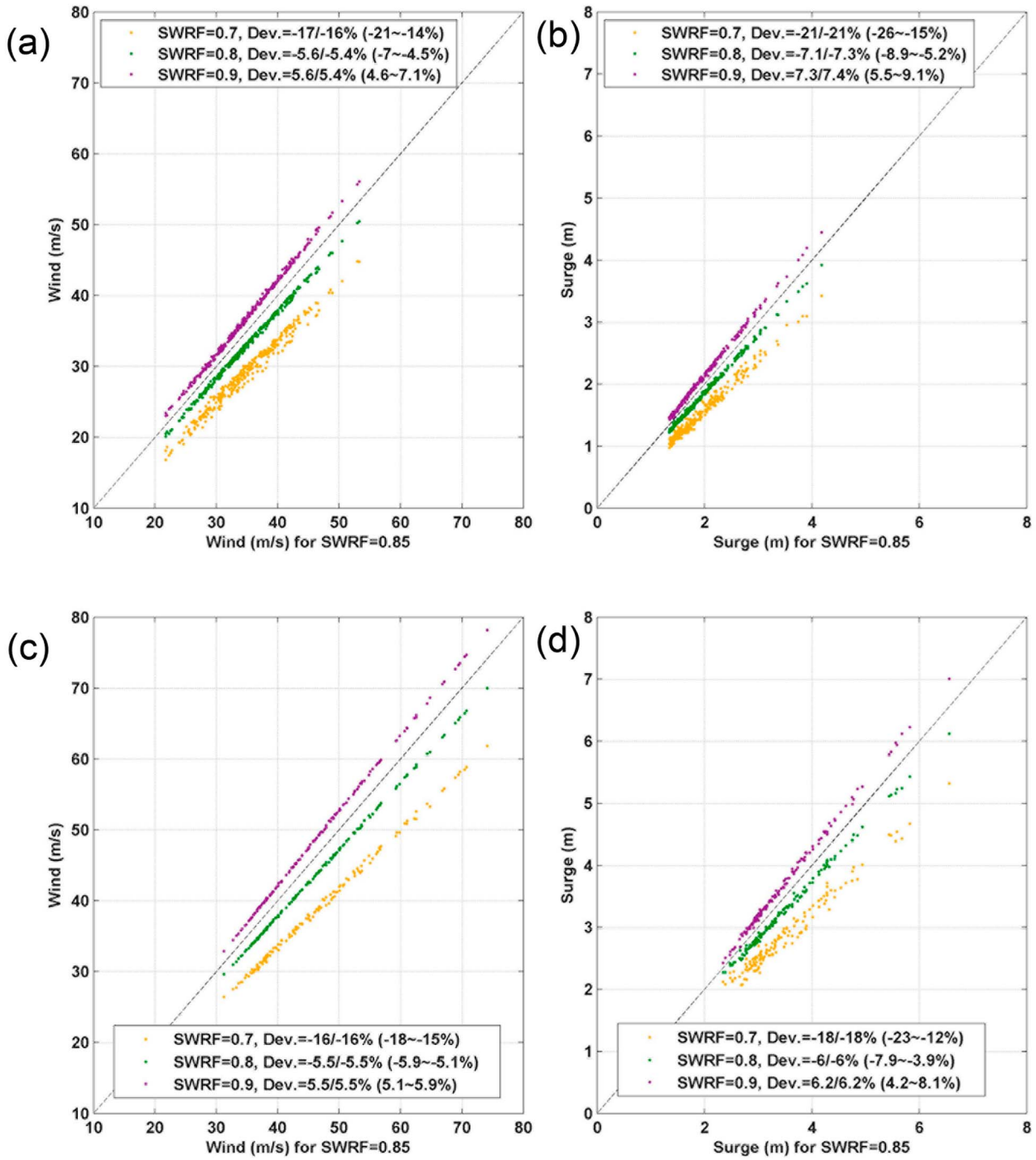

Figure 7. Comparison of the wind and surge estimates using various values of the surface wind reduction factor, SWRF, with those of the control case using SWRF = 0.85, for (a and b) NYC (295 storms) and (c and d) Tampa (135 storms).

center, over all it gives more precise estimates than the other wind profiles.

3.3. Surface Wind Adjustment

[26] In this study, the wind fields at gradient height are adjusted to the surface (at 10 m) through the use of the empirical surface wind reduction factor, SWRF, and storm inflow angle. Various values of SWRF, ranging from 0.65 to 0.95 over the ocean, have been used in the literature (a review is given by *Vickery et al.* [2009a]). As the value of SWRF is uncertain and it may also vary with the wind speed [*Powell et al.*, 2005], uncertainties in wind and surge estimates may be induced when using a SWRF. To estimate how large the uncertainties can be, we analyze the sensitivity

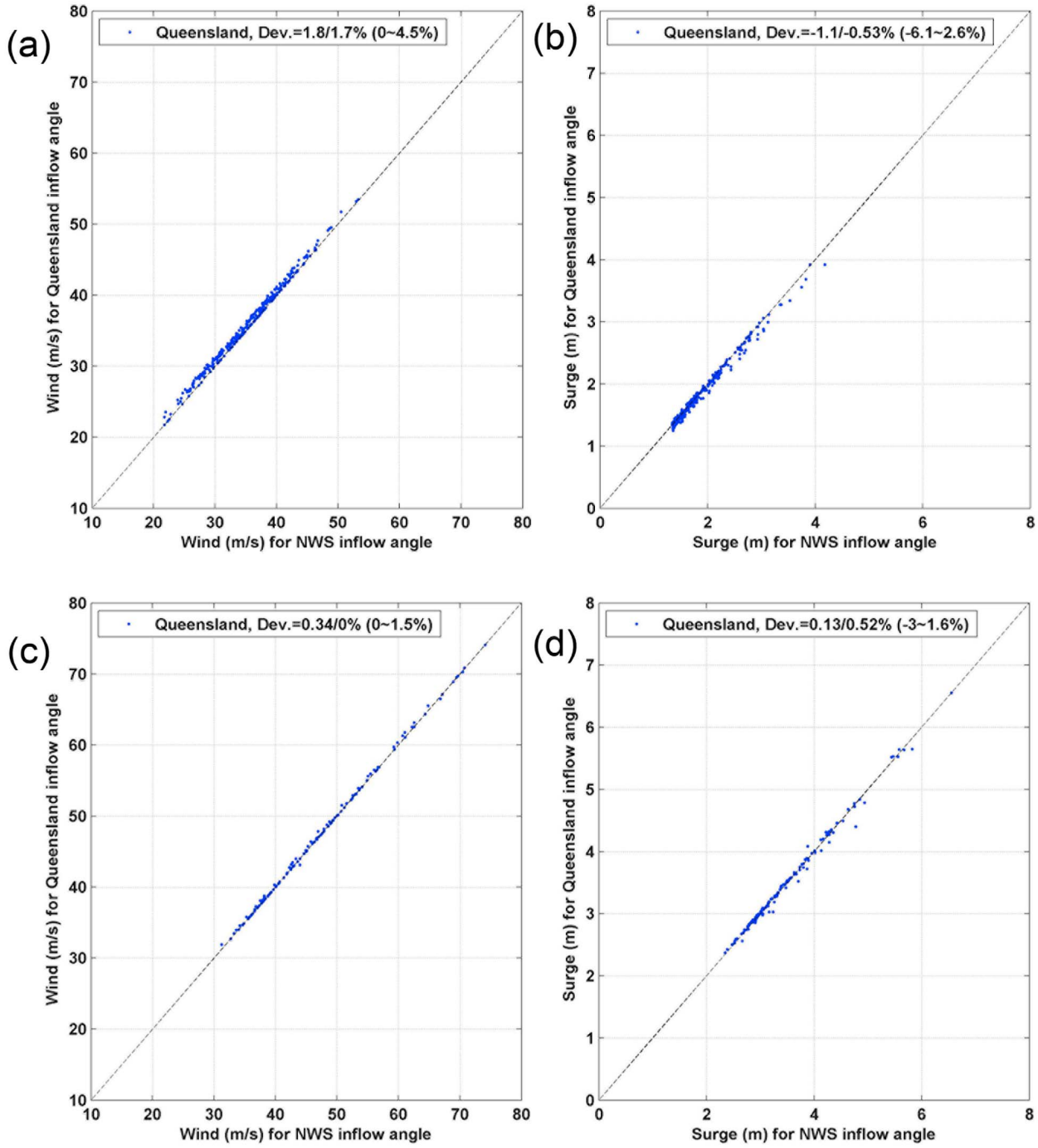

Figure 8. Comparison of the wind and surge estimates using Queensland's inflow angle with those of the control case using NWS's inflow angle, for (a and b) NYC (295 storms) and (c and d) Tampa (135 storms).

of wind and surge estimates to this parameter in the range of 0.7–0.9, as shown in Figure 7. Both wind and surge estimates change greatly with SWRF, because it directly affects the magnitude of the surface wind associated with the storm, which dominates the wind field for extreme events. Every incremental increase (decrease) of the value of SWRF by 0.05 from 0.85 increases (decreases) the magnitude of the wind speeds associated with the storm by about 5.9%, and thus it increases (decreases) the peak wind estimates by a slightly different amount, on average about 5.6% for NYC and 5.5% for Tampa (Figures 7a and 7c); this difference and the variation among storms reflect the effect of the (unchanged) background wind component. Curiously, every incremental increase (decrease) of the value of SWRF by 0.05 from 0.85 increases (decreases) the surge estimates on average by about 7% for NYC and 6% for Tampa (Figures 7b and 7d); the change of the surge is only slightly larger than the change of the wind when it is applied

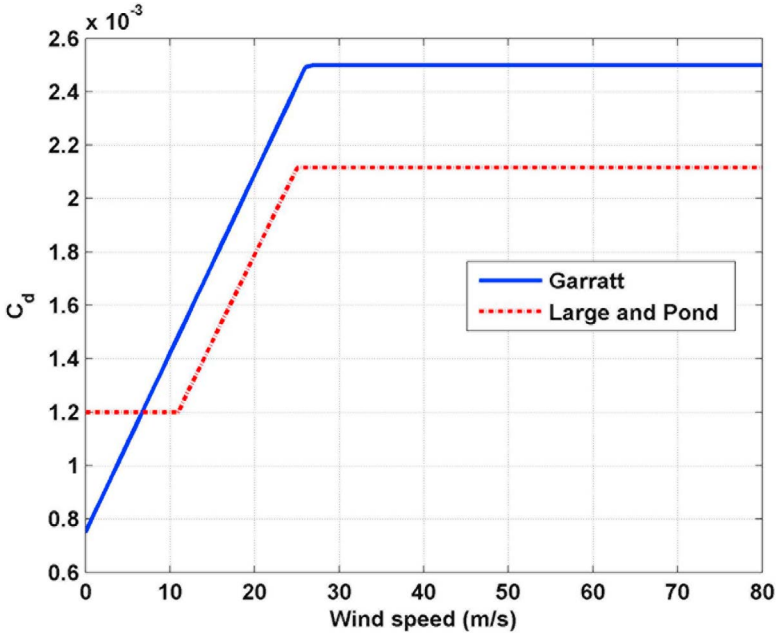

Figure 9. Sea surface drag coefficient of *Large and Pond* [1981] and *Garratt* [1977] modified based on *Powell et al.* [2003].

uniformly over the entire wind field. This nearly linear response of the surge to the wind is not observed in the analysis of surge sensitivity to different gradient wind profiles, where the wind field is varied differently over space and the change of the surge is much larger than the change of the wind (see Figures 5 and 6). The largest mean variation of the wind estimates is 27% for NYC and 26.2% for Tampa and the largest mean variation of the surge estimates is 36% for NYC and 29.6% for Tampa, due to the deviations of the estimates using SWRF = 0.9 from those using SWRF = 0.7.

[27] We identify two common empirical forms of storm inflow angle, measured inward from the azimuthal direction, as functions of the distance to the center of the storm. The NWS recommends approximating the inflow angle to increase linearly from 10° at the storm center to 20° at R_m and then to 25° at $1.2R_m$, and to remain at 25° beyond $1.2R_m$ [*Bretschneider*, 1972]. *Queensland Government* [2001] uses a somewhat different expression for the inflow angle, which increases linearly from 0° at the storm center to 10° at R_m and then to 25° at $1.2R_m$, and remains at 25° beyond $1.2R_m$. The difference between these two forms is that Queensland' inflow angle is smaller than that of NWS in the storm inner region. The sensitivities of both the wind and surge estimates to these two inflow angle representations are relatively small, as shown in Figure 8. The wind estimates using the Queensland inflow angle are slightly higher than those using the NWS inflow angle, with a mean deviation of 1.8% for NYC and 0.34% for Tampa. The surge estimates using the Queensland inflow angle, however, may be lower or higher than those using the NWS inflow angle, with a mean deviation of −1.1% for NYC and 0.13% for Tampa. This difference exists because the inflow angle of storms moving along the Atlantic coast usually enhances the transport of water into New York Harbor, while the opposite is true in Tampa Bay, which is consistent with the different effects of the background wind rotation parameter β on the two sites (see Figure 3).

3.4. Sea Surface Drag Coefficient

[28] The wind surface stress is a quadratic function of the surface wind velocity, multiplied by the air density and a sea surface drag coefficient, C_d; given the surface wind velocity, the wind stress increases linearly with C_d. We compare the surge sensitivities to the wind parameters from above with the surge sensitivities to the critical parameter C_d in surge modeling. C_d is often modeled as an increasing function of the surface wind speed; *Powell et al.* [2003], however, suggest that C_d reaches a maximum value at high wind speeds and levels off or decreases. Therefore, the C_d functions are often applied with caps. Here we compare two C_d functions. One is Garratt's drag formula [*Garratt*, 1977], which is often used in surge modeling [e.g., *Westerink et al.*, 2008], with a cap of 0.0025 according to *Powell et al.*, [2003]. The other is Large and Pond's drag formula [*Large and Pond*, 1981] with the value of C_d being capped at 0.0021 when the wind speed is greater than 25 m/s; this form is comparable to *Powell et al.*'s [2003] observations [*Vickery et al.*, 2009a]. These two drag formulae are plotted in Figure 9. Large and Pond's C_d is smaller than Garratt's C_d, except at low wind speeds (<6 m/s). The surge estimates using Large and Pond's C_d, therefore, are smaller than those using Garratt's C_d, as shown in Figure 10, with a mean deviation of −11% for NYC and −9% for Tampa. The magnitude of the surge sensitivity to these two forms of C_d is relatively large and is comparable to the magnitude of the surge sensitivity to the four gradient wind profiles (Figures 5 and 6) and to SWRF (Figure 7).

4. Pitfalls in Parametric Wind and Surge Analysis

[29] We study the uncertainties of the wind and surge estimates due to uncertainties in the wind parameters within

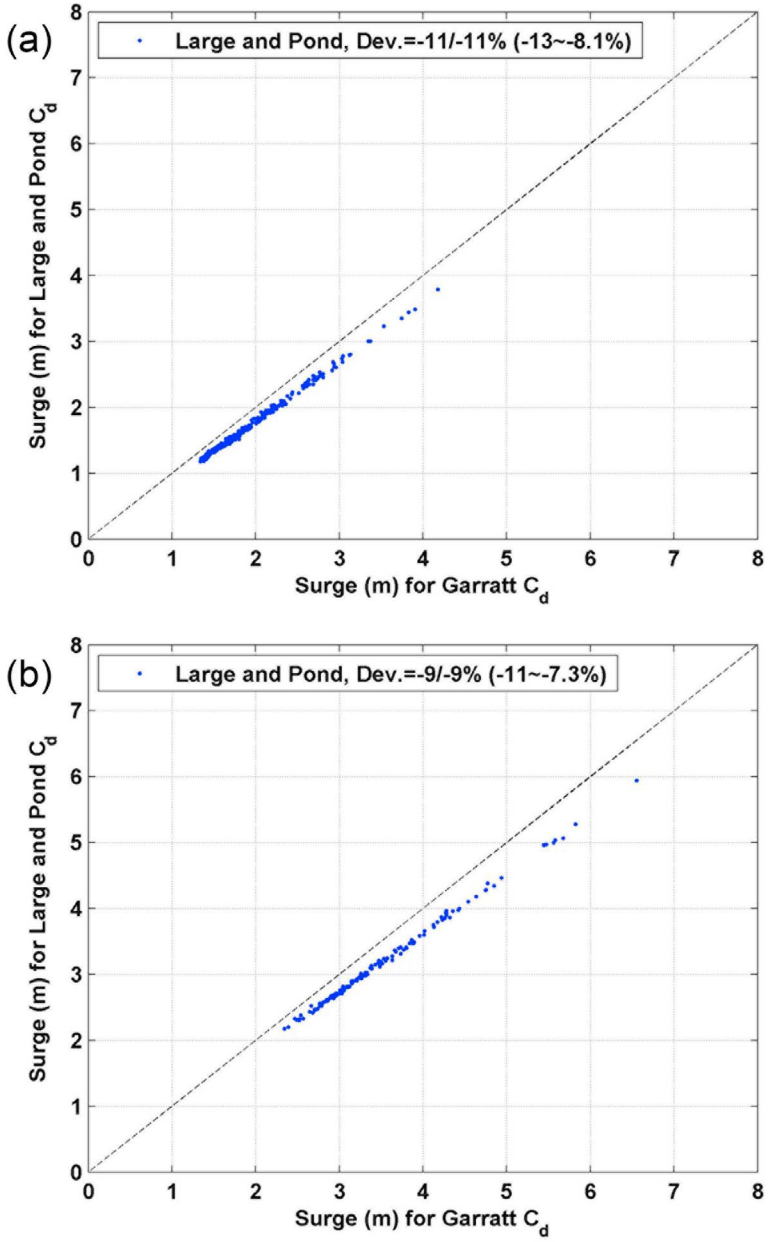

Figure 10. Comparison of the surge estimates using Large and Pond's drag coefficients with those of the control case using Garratt's drag coefficients, for (a) NYC (295 storms) and (b) Tampa (135 storms).

the ranges that are defined based on theories and observations. For both study sites, NYC and Tampa, the largest uncertainties in wind and surge estimations may be induced by uncertainties in SWRF (Figure 7), followed by the gradient wind profile (Figures 5 and 6). The surge uncertainties due to these two parameters are comparable to the surge uncertainties due to C_d (Figure 10). Here we show two examples where using wind parameters that are out of the defined ranges may lead to larger uncertainties (or errors if the parameters used are inconsistent with observation or theory).

[30] Based on the direct analysis of observations of surface wind fields and storm tracks, we suggest that the background wind is related to storm movement with a storm translation to surface background wind reduction factor, $\alpha = 0.55$, and a counter-clockwise rotation angle, $\beta = 20°$ (Section 2). Wind and surge estimates are not sensitive to the changes in these parameters within the observational ranges (0.5–0.6 and 15°–22°; Section 3.1). Here we consider two different representations of the surface background wind that are often used in practice: one neglects the velocity differences between the surface background wind and the storm translation and uses $\alpha = 1$ and $\beta = 0°$ [e.g., *Powell et al.*, 2005; *Mattocks and Forbes*, 2008; *Vickery et al.*, 2009b]; the other, used in the NWS's surge model SLOSH [*Jelesnianski et al.*, 1992], assumes that $\beta = 0°$ and α follows the SLOSH wind profile so that it is equal to zero at the center of the storm, increases to a maximum of 0.5 at the

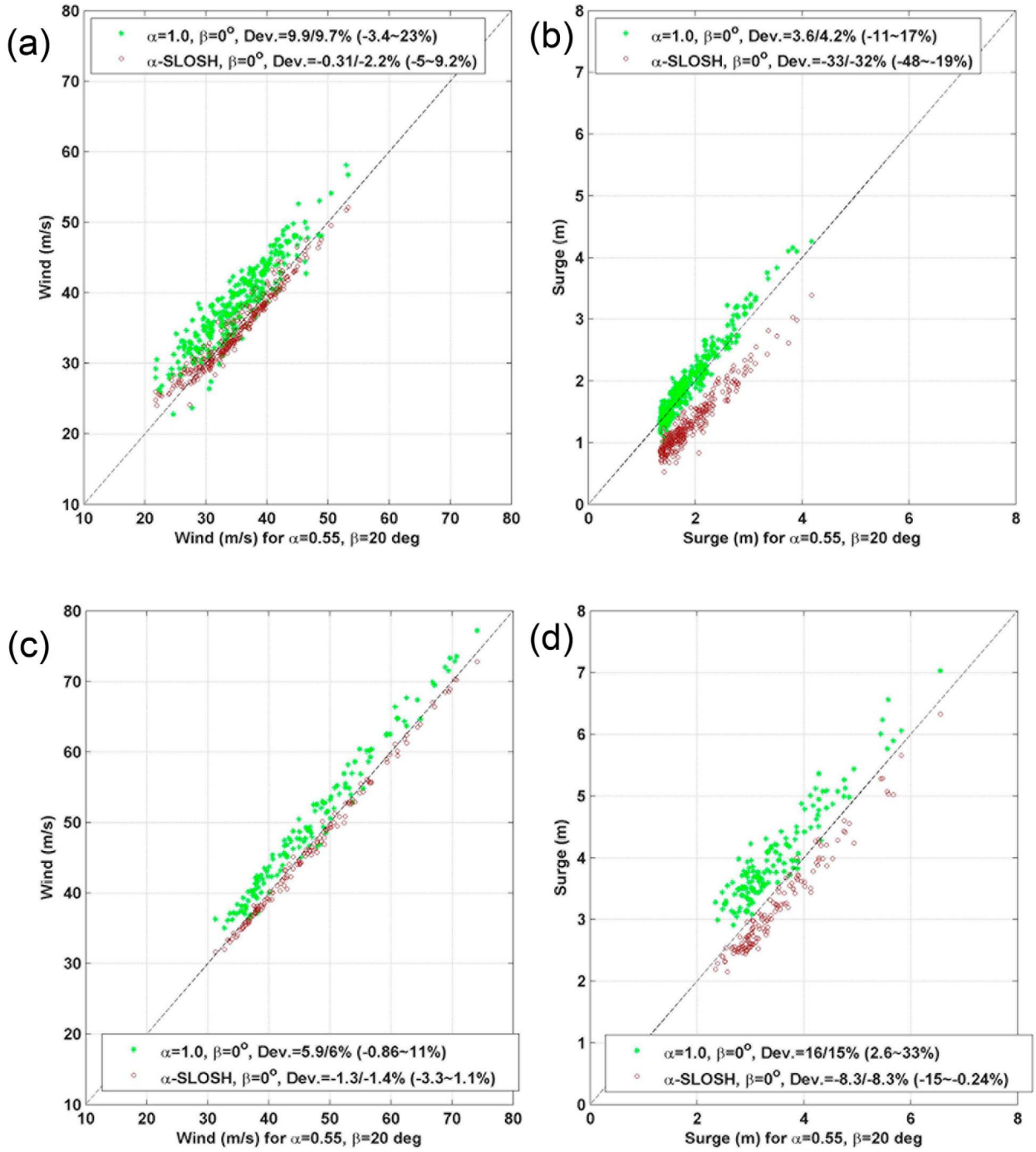

Figure 11. Comparison of the wind and surge estimates using two often-used values of the surface background wind reduction factor, α, and rotation angle, $\beta = 0°$, with those of the control case using $\alpha = 0.55$, $\beta = 20°$, for (a and b) NYC (295 storms) and (c and d) Tampa (135 storms).

radius of maximum wind, and then decreases radially outward (denoted hereafter by α-SLOSH). Although our analysis also show some radial dependence of α, α-SLOSH decreases much faster away from the radius of maximum wind and thus may greatly underestimate the background wind.

[31] Figure 11 displays the estimated peak winds and surges at NYC and Tampa using these two representations of the background wind, compared to those using (α, β) = (0.55, 20°). For the surge estimates, as shown in Figures 3b and 3d, a larger value of α typically increases surge, whereas a larger value of β increases surge for NYC but decreases surge for Tampa. Also, the change with α dominates the change with β for the considered cases. Therefore, compared to the results using (α, β) = (0.55, 20°), using (α, β) = (1, 0°)

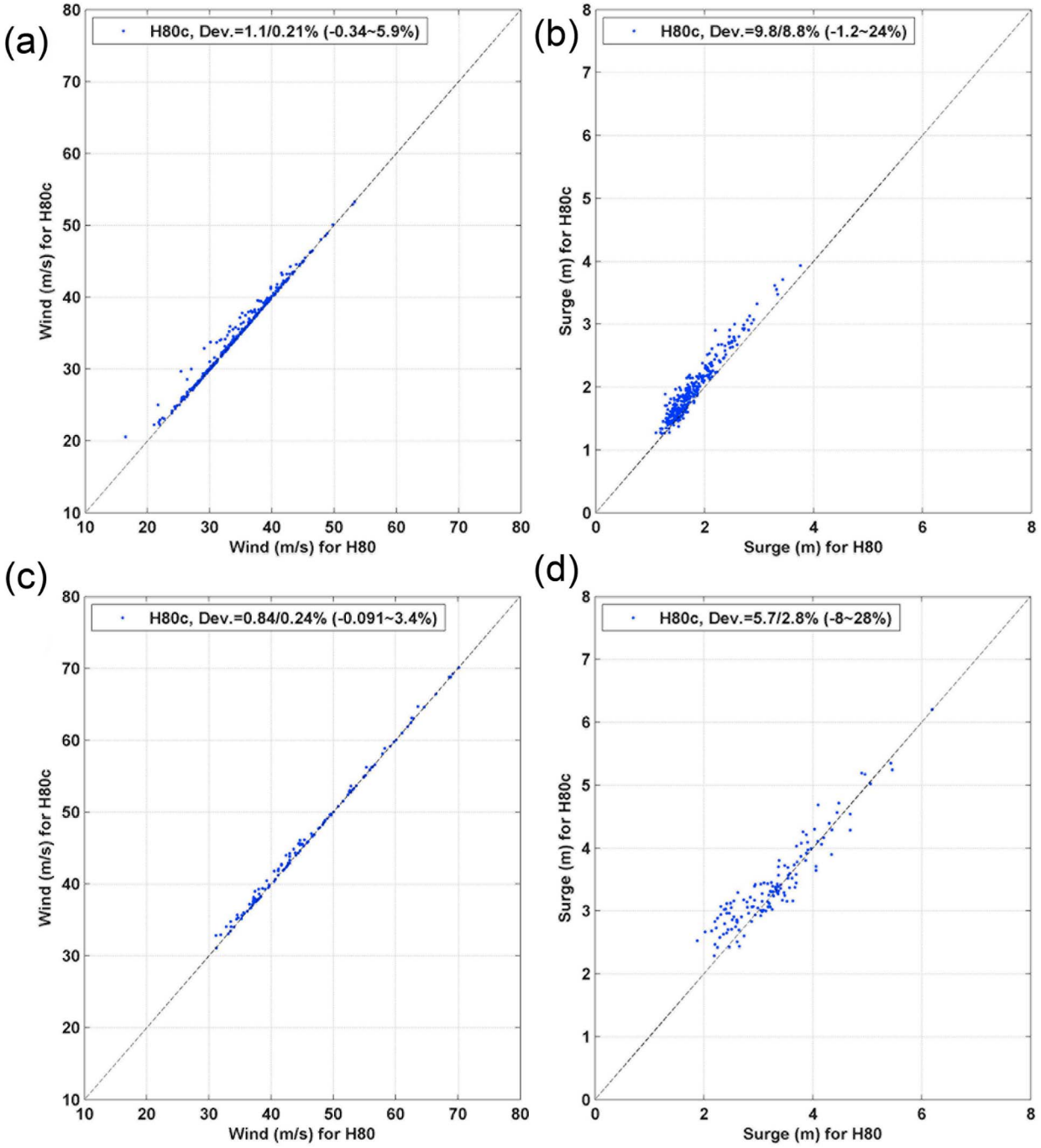

Figure 12. Comparison of the wind and surge estimates using the cyclostrophic approximation of H80 profile, H80c, with those using the H80 profile, for (a and b) NYC (295 storms) and (c and d) Tampa (135 storms).

overestimates the surge significantly for Tampa (with a mean deviation of 16%) but moderately for NYC (3.6%); using (α, β) = (α-SLOSH, 0°) underestimates the surge significantly for NYC (-33%) but moderately for Tampa (-8.3%). For the wind estimates, although Figures 3a and 3c show that the winds are often increased by increasing either α or β in the observed ranges, it is difficult to explain the mechanism by which β affects the peak winds at the sites; neglecting β may induce relatively small under- or even over-estimation in the winds. Thus using (α, β) = (α-SLOSH, 0°) underestimates the winds only slightly (-0.31% for NYC and -1.3% for Tampa) while using (α, β) = (1, 0°) overestimates the winds more significantly (9.9% for NYC and 5.9% for Tampa); the

differences are mainly due to the different changes in α from the control case, especially in the regions close to the maximum winds (0.5 versus 0.55 and 1 versus 0.55). These analyses demonstrate that applying the often-used representations of the surface background wind, with (α, β) = (1, 0°) or (α, β) = (α-SLOSH, 0°), may induce large errors in wind and especially surge estimates; the magnitudes of the estimation errors can be much larger than the magnitudes of the estimation uncertainties due to the variations of any of the wind parameters (and C_d) that we have discussed. Using the observed mean values of α (about 0.55) and β (about 20°) will give more accurate estimates of the wind and surge on average, although uncertainties exist for individual storms.

[32] The wind and surge estimates are also very sensitive to the wind profiles (Figures 5 and 6), and thus unnecessary approximations in the wind profiles should be avoided. As discussed in Section 3.2, using the cyclostrophic form of the Holland profile H80, H80c, may overestimate the wind speed away from the radius of maximum wind (see Figure 4) and thus induce inaccurate estimation of the peak wind and surge at the sites. Figure 12 compares the winds and surges estimated using H80c with those estimated using H80 for NYC and Tampa. H80c overestimates the wind only slightly (by a mean deviation of about 1.1% for NYC and 0.84% for Tampa) as the peak wind at the sites is often generated from the wind field close to the radius of maximum wind. However, H80c may significantly overestimate the surge (9.8% for NYC and 5.7% for Tampa) as the surge is also affected by the wind field away from the radius of maximum wind. Thus, the magnitudes of errors induced by the cyclostrophic approximation are comparable to the magnitudes of uncertainties that result from using various wind profiles (Figures 5 and 6); H80c should not be applied in wind and especially not in surge analysis.

5. Conclusions

[33] Hurricane wind and surge analyses are greatly influenced by the details of the total near-surface wind field. Parametric wind field modeling is widely applied to wind and surge predictions, especially for long-term risk assessment. The parametric surface wind field may be estimated as the sum of a storm-wind component and a background-wind component. Analyzing the observed surface wind fields and storm tracks, we found that, with relatively small spatial variations, the surface background wind on average was reduced in magnitude from the storm translation velocity by a factor of about 0.55 (α) and was rotated in the counterclockwise direction by about 20° (β). These estimates differ significantly from the values used in current wind and surge analysis.

[34] The wind field associated with the storm is determined by the storm gradient wind profile and the effect of surface friction, which is represented by the surface wind reduction factor, SWRF, and inflow angle. We carried out numerical simulations to investigate the sensitivities of the peak wind and surge estimates to the uncertainties in these wind parameters plus α and β. We also estimated the sensitivity of the surge estimates to the uncertainty in the sea surface drag coefficient, C_d, for comparison. The main findings, for two study sites (NYC and Tampa) and for extreme storms (with return periods greater than 50 years), are as follows:

[35] 1. Although some uncertainties exist in the estimations of α and β, the wind and surge estimates are not sensitive to their observed radial-variation ranges of 0.5–0.6 and 15°–22°, respectively; the uncertainties in the wind and surge estimates on average (over all the extreme storms) are less than 1.3% and 4%, respectively.

[36] 2. The wind and surge estimates are relatively sensitive to the uncertainty in the gradient wind profile. The variations in the wind and surge estimates due to the variations in the four wind profiles in this study [*Holland*, 1980; *Jelesnianski et al.*, 1992; *Emanuel*, 2004; *Emanuel and Rotunno*, 2011] are on average up to 5% and 21.7%, respectively. *Emanuel and Rotunno*'s [2011] wind profile, E11, is most likely to give accurate estimates (for both wind and surge) compared to the other wind profiles. Compared to those using E11, the wind and surge estimates using the other wind profiles may on average be lower by up to 4% and 13%, respectively, or higher by up to 0.6% and 5.4%, respectively.

[37] 3. The wind and surge estimates are very sensitive to the uncertainty in SWRF, but the estimates vary almost linearly with SWRF in the observational range of 0.7–0.9; on average, every increase (decrease) of the value of SWRF by 0.05 from 0.85 increases (decreases) the wind estimates at the sites by about 5.5% and the surge estimates by about 6%–7%. The variations in the wind and surge estimates due to the variation of SWRF between 0.7 and 0.9 can be on average as large as about 27% and 36%, respectively.

[38] 4. The wind and surge estimates are not sensitive to the two forms of inflow angle investigated [*Bretschneider*, 1972; *Queensland Government*, 2001], with average uncertainties in the estimates of less than about 2% and 1%, respectively.

[39] 5. The sensitivities of the surge estimates to the uncertainties in wind profiles and SWRF are comparable to the surge sensitivity to the uncertainty in the critical surge-modeling parameter C_d. The surge estimates using *Large and Pond*'s [1981] C_d are about 10% smaller than those using *Garratt*'s [1977] C_d (capped by 0.0025).

[40] It is important to note that the uncertainties of the wind and surge estimates noted above are induced by the uncertainties in the wind parameters within the ranges that are defined based on theories and observations. Parametric wind modeling and surge analysis must be done with caution because using wind parameters inconsistent with observations or theory may lead to errors with larger amplitudes. In particular, two commonly used representations of the surface background wind, with (α, β) = (1, 0°) and (α, β) = (α-SLOSH, 0°), may induce errors with average magnitudes up to 10% for wind estimates and up to 33% for surge estimates. Also, the cyclostrophic approximation of the *Holland* [1980] wind profile may overestimate the surge by an average magnitude as large as 10%, compared to the gradient wind-balance form of the profile. Such significant errors should be avoided in future hurricane wind and surge predictions, risk assessment, and uncertainty analysis.

[41] **Acknowledgments.** N.L. was supported by the NOAA Climate and Global Change Postdoctoral Fellowship Program, administered by the University Corporation for Atmospheric Research. D.C. was supported by the Department of Energy Office of Science Graduate Fellowship Program

(DOE SCGF), made possible in part by the American Recovery and Reinvestment Act of 2009, administered by ORISE-ORAU under contract DE-AC05-06OR23100. We thank Kerry Emanuel of Massachusetts Institute of Technology for providing us with the synthetic storm data sets and for his advice and suggestions on this study. We also thank Joannes Westerink of the University of Notre Dame for providing us with guidance in creating the ADCIRC mesh for Tampa.

References

Batts, M. E., M. R. Cordes, L. R. Russell, J. R. Shaver, and E. Simiu (1980), Hurricane wind speeds in the United States, *Rep. BSS-124*, Natl. Bur. of Stand., U.S. Dep. of Commer., Washington, D. C.

Blain, C. A., J. J. Westerink, and R. A. Luettich (1994), The influence of domain size on the response characteristics of a hurricane storm surge model, *J. Geophys. Res.*, *99*(C9), 18,467–18,479, doi:10.1029/94JC01348.

Bretschneider, C. L. (1972), A non-dimensional stationary hurricane wave model, paper presented at the Offshore Technology Conference, Am. Inst. of Min., Metal., and Pet. Eng., Houston, Texas.

Bunya, S., et al. (2010), A high-resolution coupled riverine flow, tide, wind, wind wave, and storm surge model for southern Louisiana and Mississippi. Part I: Model development and validation, *Mon. Weather Rev.*, *138*, 345–377, doi:10.1175/2009MWR2906.1.

Chan, J. C. L. (2005), The physics of tropical cyclone motion, *Annu. Rev. Fluid Mech.*, *37*, 99–128, doi:10.1146/annurev.fluid.37.061903.175702.

Chavas, D. R., and K. A. Emanuel (2010), A QuikSCAT climatology of tropical cyclone size, *Geophys. Res. Lett.*, *37*, L18816, doi:10.1029/2010GL044558.

Colle, B. A., F. Buonaiuto, M. J. Bowman, R. E. Wilson, R. Flood, R. Hunter, A. Mintz, and D. Hill (2008), New York City's vulnerability to coastal flooding, *Bull. Am. Meteorol. Soc.*, *89*, 829–841, doi:10.1175/2007BAMS2401.1.

Emanuel, K. (2004), Tropical cyclone energetics and structure, in *Atmospheric Turbulence and Mesoscale Meteorology*, edited by E. Fedorovich, R. Rotunno, and B. Stevens, pp. 165–192, Cambridge Univ. Press, Cambridge, U. K., doi:10.1017/CBO9780511735035.010.

Emanuel, K., and R. Rotunno (2011), Self-stratification of tropical cyclone outflow. Part I: Implications for storm structure, *J. Atmos. Sci.*, *68*, 2236–2249. doi:http://dx.doi.org/10.1175/JAS-D-10-05024.1

Emanuel, K., S. Ravela, E. Vivant, and C. Risi (2006), A statistical deterministic approach to hurricane risk assessment, *Bull. Am. Meteorol. Soc.*, *87*, 299–314, doi:10.1175/BAMS-87-3-299.

Emanuel, K., R. Sundararajan, and J. Williams (2008), Hurricanes and global warming: Results from downscaling IPCC AR4 simulations, *Bull. Am. Meteorol. Soc.*, *89*, 347–367, doi:10.1175/BAMS-89-3-347.

Flather, R. A. (2001), Storm surges, in *Encyclopedia of Ocean Sciences*, edited by J. H. Steele, S. A. Thorpe, and K. K. Turekian, pp. 2882–2892, Academic, San Diego, Calif., doi:10.1006/rwos.2001.0124

Frank, W. M., and E. A. Ritchie (1999), Effects on environmental flow upon tropical cyclone structure, *Mon. Weather Rev.*, *127*, 2044–2061, doi:10.1175/1520-0493(1999)127<2044:EOEFUT>2.0.CO;2.

Garratt, J. R. (1977), Review of drag coefficients over oceans and continents, *Mon. Weather Rev.*, *105*, 915–929, doi:10.1175/1520-0493(1977)105<0915:RODCOO>2.0.CO;2.

Holland, G. J. (1980), An analytic model of the wind and pressure profiles in hurricanes, *Mon. Weather Rev.*, *108*, 1212–1218, doi:10.1175/1520-0493(1980)108<1212:AAMOTW>2.0.CO;2.

Holland, G. J., J. I. Belanger, and A. Fritz (2010), A revised model for radial profiles of hurricane winds, *Mon. Weather Rev.*, *138*, 4393–4401, doi:10.1175/2010MWR3317.1.

Houston, S. H., W. A. Shaffer, M. D. Powell, and J. Chen (1999), Comparisons of HRD and SLOSH surface wind fields in hurricanes: Implications for storm surge modeling, *Weather Forecast.*, *14*, 671–686, doi:10.1175/1520-0434(1999)014<0671:COHASS>2.0.CO;2.

Irish, J. L., D. T. Resio, and J. J. Ratcliff (2008), The Influence of storm size on hurricane surge, *J. Phys. Oceanogr.*, *38*, 2003–2013, doi:10.1175/2008JPO3727.1.

Jarvinen, B. R., C. J. Neumann, and M. A. S. Davis (1984), A tropical cyclone data tape for the North Atlantic basin, 1886–1983: Contents, limitations, and uses, *NOAA Tech. Memo NWS NHC 22*, NOAA Trop. Predict. Cent., Miami, Fla.

Jelesnianski, C. P. (1966), Numerical computations of storm surges without bottom stress, *Mon. Weather Rev.*, *94*(6), 379–394, doi:10.1175/1520-0493(1966)094<0379:NCOSSW>2.3.CO;2.

Jelesnianski, C. P., J. Chen, and W. A. Shaffer (1992), SLOSH: Sea, lake, and overland surges from hurricanes, *NOAA Tech. Rep. NWS 48*, NOAA AOML Library, Miami, Fla.

Kalnay, E., et al. (1996), The NCEP/NCAR 40-year reanalysis project, *Bull. Am. Meteorol. Soc.*, *77*, 437–471, doi:10.1175/1520-0477(1996)077<0437:TNYRP>2.0.CO;2.

Kepert, J. D. (2010), Slab- and height-resolving models of the tropical cyclone boundary layer. Part I: Comparing the simulations, *Q. J. R. Meteorol. Soc.*, *136*, 1686–1699, doi:10.1002/qj.667.

Kurihara, Y., R. E. Tuleya, and M. A. Bender (1998), The GFDL hurricane prediction system and its performance in the 1995 hurricane season, *Mon. Weather Rev.*, *126*, 1306–1322, doi:10.1175/1520-0493(1998)126<1306:TGHPSA>2.0.CO;2.

Large, W. G., and S. Pond (1981), Open ocean momentum flux measurements in moderate to strong winds, *J. Phys. Oceanogr.*, *11*, 324–336, doi:10.1175/1520-0485(1981)011<0324:OOMFMI>2.0.CO;2.

Lin, N., J. A. Smith, G. Villarini, T. P. Marchok, and M. L. Baeck (2010a), Modeling extreme rainfall, winds, and surge from Hurricane Isabel (2003), *Weather Forecast.*, *25*, 1342–1361, doi:10.1175/2010WAF2222349.1.

Lin, N., K. A. Emanuel, J. A. Smith, and E. Vanmarcke (2010b), Risk assessment of hurricane storm surge for New York City, *J. Geophys. Res.*, *115*, D18121, doi:10.1029/2009JD013630.

Lin, N., K. Emanuel, M. Oppenheimer, and E. Vanmarcke (2012), Physically based assessment of hurricane surge threat under climate change, *Nat. Clim. Change*, doi:10.1038/nclimate1389, in press.

Luettich, R. A., J. J. Westerink, and N. W. Scheffner (1992), ADCIRC: An advanced three-dimensional circulation model for shelves, coasts, and estuaries. Report 1: Theory and methodology of ADCIRC-2DDI and ADCIRC-3DL, *Dredging Res. Program Tech. Rep. DRP-92-6*, Coastal Eng. Res. Cent., Vicksburg, Miss.

Mattocks, C., and C. Forbes (2008), A real-time, event-triggered storm surge forecasting system for the state of North Carolina, *Ocean Modell.*, *25*, 95–119, doi:10.1016/j.ocemod.2008.06.008.

Phadke, A. C., C. D. Martino, K. F. Cheung, and S. H. Houston (2003), Modeling of tropical cyclone winds and waves for emergency management, *Ocean Eng.*, *30*, 553–578, doi:10.1016/S0029-8018(02)00033-1.

Powell, M., S. Houston, and T. Reinhold (1996), Hurricane Andrew's landfall in south Florida. Part I: Standardizing measurements for documentation of surface wind fields, *Weather Forecast.*, *11*, 304–328, doi:10.1175/1520-0434(1996)011<0304:HALISF>2.0.CO;2.

Powell, M. D., S. H. Houston, L. R. Amat, and N. Morisseau-Leroy (1998), The HRD real-time hurricane wind analysis system, *J. Wind Eng. Indust. Aerodyn.*, *77/78*, 53–64, doi.org/10.1016/S0167-6105(98)00131-7.

Powell, M. D., P. J. Vickery, and T. A. Reinhold (2003), Reduced drag coefficient for high wind speeds in tropical cyclones, *Nature*, *422*(6929), 279–283, doi:10.1038/nature01481.

Powell, M. D., G. Soukup, S. Cocke, S. Gulati, N. Morisseau-Leroy, S. Hamid, N. Dorst, and L. Axe (2005), State of Florida hurricane loss projection model: Atmospheric science component, *J. Wind Eng. Ind. Aerodyn.*, *93*, 651–674, doi:10.1016/j.jweia.2005.05.008.

Queensland Government (2001), Queensland climate change and community vulnerability to tropical cyclones: Ocean hazards assessment - stage 1, *J0004–PR0001C*, 383 pp., Dep. of Nat. Resour. and Mines, Brisbane, Queensl., Australia.

Rego, J. L., and C. Li (2009), On the importance of the forward speed of hurricanes in storm surge forecasting: A numerical study, *Geophys. Res. Lett.*, *36*, L07609, doi:10.1029/2008GL036953.

Shea, D. J., and W. M. Gray (1973), The hurricane's inner core region. I. Symmetric and asymmetric structure, *J. Atmos. Sci.*, *30*, 1544–1564, doi.org/10.1175/1520-0469(1973)030<1544:THICRI>2.0.CO;2

Thompson, E. F., and V. J. Cardone (1996), Practical modeling of hurricane surface wind fields, *J. Waterw. Port Coastal Ocean Eng.*, *122*, 195–205, doi:10.1061/(ASCE)0733-950X(1996)122:4(195).

Vickery, P. J., P. F. Skerjl, and L. A. Twisdale (2000), Simulation of hurricane risk in the U.S. using empirical track model, *J. Struct. Eng.*, *126*, 1222–1237, doi:10.1061/(ASCE)0733-9445(2000)126:10(1222).

Vickery, P. J., F. J. Masters, M. D. Powell, and D. Wadhera (2009a), Hurricane hazard modeling: The past, present, and future, *J. Wind Eng. Ind. Aerodyn.*, *97*, 392–405, doi:10.1016/j.jweia.2009.05.005.

Vickery, P. J., D. Wadhera, M. D. Powell, and Y. Chen (2009b), A hurricane boundary layer and wind field model for use in engineering applications, *J. Appl. Meteorol. Climatol.*, *48*, 381–405, doi:10.1175/2008JAMC1841.1.

Weatherford, C. L., and W. M. Gray (1988), Typhoon structure as revealed by aircraft reconnaissance. Part II: Structural variability, *Mon. Weather Rev.*, *116*, 1044–1056, doi:10.1175/1520-0493(1988)116<1044:TSARBA>2.0.CO;2.

Weisberg, R. H., and L. Zheng (2006), Hurricane storm surge simulations for Tampa Bay, *Estuaries Coasts*, *29*, 899–913.

Westerink, J. J., R. A. Luettich, C. A. Blain, and N. W. Scheffner (1992), ADCIRC: An advanced three-dimensional circulation model for shelves,

coasts, and estuaries, report 2: User's manual for ADCIRC-2DDI, *Dredging Res. Program Tech. Rep. DRP-92–6*, Coastal Eng. Res. Cent., Vicksburg, Miss.

Westerink, J. J., J. C. Feyen, J. H. Atkinson, H. J. Roberts, E. J. Kubatko, R. A. Luettich, C. Dawson, M. D. Powell, J. P. Dunion, and H. Pourtuheri (2008), A basin- to channel- scale unstructured grid hurricane storm surge model applied to southern Louisiana, *Mon. Weather Rev.*, *136*, 833–864, doi:10.1175/2007MWR1946.1.

Yankovsky, A. E. (2009), Large-scale edge waves generated by hurricane landfall, *J. Geophys. Res.*, *114*, C03014, doi:10.1029/2008JC005113.